The Role of Ruthenium and Rhenium Diimine Complexes in Conjugated Polymers That Exhibit Interesting Opto-Electronic Properties

Po King Ng, Xiong Gong, Suk Hang Chan, Lillian Sze Man Lam, and Wai Kin Chan*[a]

Abstract: This paper reports the synthesis and opto-electronic properties of different conjugated polymers that contain the diimine complexes of ruthenium or rhenium. Conjugated poly(phenylene vinylene)s that contain aromatic 1,3,4-oxadiazole and 2,2′-bipyridine units on the main chain were synthesized by the palladium catalyzed olefinic coupling reaction. Other types of polymers based on 1,10-phenanthroline bis(2,2-bipyridyl) ruthenium(II) or chlorotricarbonyl rhenium(I) complexes were also synthesized by the same reaction. In general, these polymers exhibit two absorption bands due to the $\pi-\pi^*$ transition of the conjugated main chain and the $d-\pi^*$ metal-to-ligand charge-transfer transition of the metal complex. As a result, the photosensitivity of the polymers beyond 500 nm was enhanced. Charge-carrier mobility measurements showed that the presence of metal complexes could facilitate the charge-transport process, and the enhancement in carrier mobility was dependent on the metal content in the polymer. In addition, we have also demonstrated that the ruthenium complex could act as both photosensitizer and light emitter. Photovoltaic cells were constructed, and they were subjected to irradiation with a xenon arc lamp. Under illumination, the short circuit current and the open circuit voltage were measured to be $0.05\ mA\,cm^{-2}$ and 0.35 V, respectively. The polymers were fabricated into single-layer emitting devices, and light emission was observed when the device was subjected to forward bias. The maximum luminance was determined to be $300\ cd\,m^{-2}$, and the external quantum efficiency was approximately 0.05 to 0.2%. Although the efficiency was relatively low when compared with other devices based on organic materials, we have demonstrated the first examples of using transition metal complexes for both photovoltaic and light-emitting applications.

Keywords: luminescence · N ligands · rhenium · ruthenium · sensitizers

Introduction

Polymer metal complexes have remarkably specific structures, in which central metal ions are surrounded by an enormous polymer chain. They show interesting and important characteristics, especially catalytic activities different from the corresponding ordinary metal complexes of low molecular weight. Moreover, they also find potential applications in many important systems such as polymer-coated electrodes, solar energy conversion, and chemical sensors and so on.[1] Since the discovery of the first organic light-emitting poly(*p*-phenylene vinylene) (PPV),[2] there has been tremendous advancement in this area in terms of material design, device fabrication, emission wavelength, and performance improvement in organic polymeric light-emitting diodes (LED).[3] Besides light-emitting properties, conjugated polymers also demonstrated various interesting electronic and photonic properties, which are comparable to traditional inorganic semiconductors. It has been reported that PPVs have been used as laser materials,[4] photodiodes,[5] and organic transistors.[6] Most of the opto-electronic polymers reported to date are based on pure organic conjugated systems, in which different kinds of functional groups are attached.[7] Our group has been continuously investigating the syntheses and properties of some conjugated polymers or polymer composites that contain ruthenium or rhenium polypyridine complexes.[8] The complexes were able to enhance the charge-carrier mobilities of the polymers by acting as extra charge carriers, and the mobilities were found to be dependent on the metal complex content. In addition, these transition metal complexes exhibit interesting electronic and excited-state properties. As a result, by incorporating metal complexes into the organic π-conjugated polymers, it is possible to tune the photosensitivity, charge transport, and electroluminescence (EL) activities of the resulting polymers. The use of tris(2,2′-bipyridyl) ruthenium(II) $[Ru(bpy)_3]^{2+}$ or 2,2′-bipyridyl rhenium(I) tricarbonyl complexes and their derivatives as light absorption or emission sensitizers in

[a] Dr. W. K. Chan, Dr. P. K. Ng, Dr. X. Gong, S. H. Chan, L. S. M. Lam
Department of Chemistry, University of Hong Kong
Pokfulam Road (Hong Kong)
Fax: (+852) 2857-1586
E-mail: waichan@hkucc.hku.hk

© WILEY-VCH Verlag GmbH, D-69451 Weinheim, 2001
0947-6539/01/0720-4358 $ 17.50+.50/0

polymers constitutes one example.[9] These d^6 transition metal complexes exhibit characteristic long-lived metal-to-ligand charge-transfer (MLCT) excited states, which can undergo different photochemical or photophysical processes. The excited metal complexes may serve as good energy donors, electron donors, or electron acceptors. One of the most promising potentials of these complexes is the conversion of solar radiation into chemical energy.[10] Conjugated polymers incorporated with these complexes have been reported in the literature.[11] It was also proposed that these complexes were able to participate in the charge-transport processes.[8a, 12] In addition, they exhibit interesting luminescence properties originated from the MLCT states. Light-emitting devices based on ruthenium, rhenium, or other transition metal complexes have also been constructed.[13] It was suggested that by utilizing the emission from the triplet excited states of transition metal complexes, the theoretical maximum quantum efficiency of the resulting light-emitting device could exceed 25% induced by light emission from singlet excitons.[14]

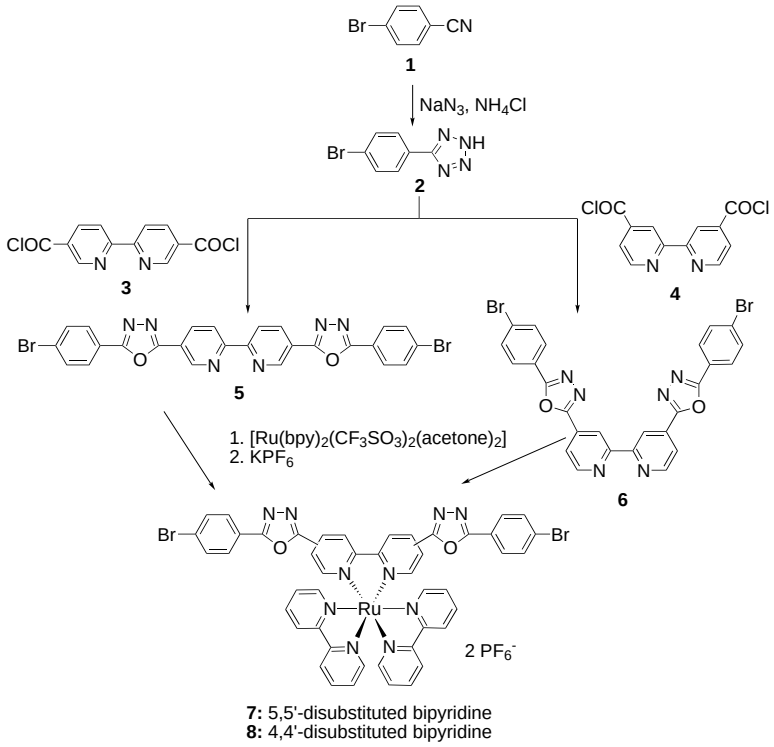

Scheme 1. Synthesis of ruthenium complexes with oxadiazole-substituted bipyridine ligands.

In this paper, we describe the synthesis, photosensitization, and light-emitting properties of a novel type of conjugated polymers, which contain a tris(2,2′-bipyridyl)ruthenium(II) type complex as the photosensitizer and light emitter. Aromatic oxadiazoles were proposed to be good candidates for advanced materials and were used in many multilayered light-emitting devices as electron-transport or hole-blocking layers.[15] They were used to enhance the electron-carrier mobility and to facilitate the charge separation after the photosensitization process. It has been shown that conjugate polymers with aromatic oxadiazole moieties exhibit improved light-emitting device performance because of the balanced charge injections from both electrodes.[16] Our objective is to investigate the roles played by these metal complexes when they are incorporated into conjugated polymer systems. This paper reports the results.

Results and Discussion

Syntheses of monomers and polymers: Ligands **5** and **6** were synthesized by the reaction between the corresponding 2,2′-bipyridinedicarbonyl chlorides **3** or **4** and 1-bromo-4-tetrazoyl-benzene **2** in excellent yield (Scheme 1).[17] Reaction of the ligands with the triflate salt of bis(2,2′-bipyridine)ruthenium(II) afforded monomers **7** or **8** in good yield. We chose hexafluorophosphate as the counter anion because its salts have higher solubility than halides in organic solvents, and they are electrochemically inert such that they do not affect the electronic or other charge-transport processes in the polymer. The syntheses of the ruthenium and rhenium complexes of 3,8-dibromo-1,10-phenanthroline (**10** and **11**) are quite straightforward. Complex **11** was prepared by refluxing the diimine ligand with rhenium pentacarbonyl chloride in toluene in high yield (Scheme 2).

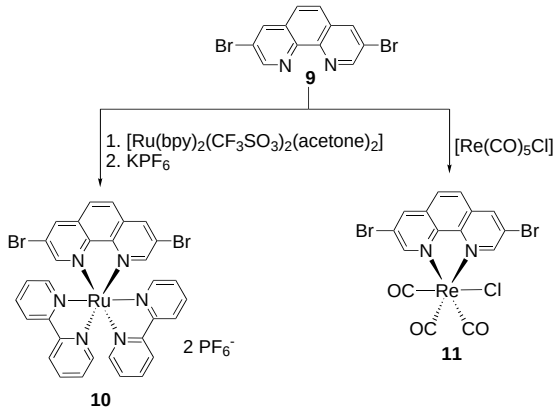

Scheme 2. Synthesis of ruthenium and rhenium complexes derived from 3,8-dibromo-1,10-phenanthroline.

Polymerization was carried out by the palladium catalyzed Heck coupling reaction by using 1,4-divinylbenzene and 1,4-dibromo-2,5-dioctoxybenzene as the comonomers. We have employed this reaction in the syntheses of different conjugated polymers functionalized with a variety of transition

metal complexes. By using this reaction, various oxophilic or electrophilic functional groups were able to survive in the polymerization reaction. Both the ruthenium and rhenium complexes were robust in these reactions. No ligand exchange reaction was observed in any one of these polymers. The metal content in the polymer can be easily adjusted by changing the proportion of the monomer metal complexes and other monomers. Both the oxadiazole based (**7** and **8**) or phenanthroline based monomers (**10** and **11**) yielded polymers in good yield. For each series of polymers, polymers with different metal content were synthesized, and the results are summarized in Tables 1 and 2.

Spectroscopic properties: The ^{1}H NMR spectra of ligand **5**, ruthenium complex **7**, and polymer **15e** are shown in Figure 1. With reference to the NMR spectra of similar bis(2,2′-bipyridyl)ruthenium complexes,[8a] the NMR spectra of **5** and **7** (Figure 1a and b) clearly agree with their structures. In Figure 1c, the spectra features of the polymer also agree with the proposed structure. The signals at approximately $\delta = 8.2-9.4$ correspond to the protons on the bipyridyl moieties, while the peaks at $\delta = 7.5-8.1$ are due to the phenylene–vinylene units. The peaks at $\delta = 4.2$, 1.9, 1.3–1.4, and 0.9 are attributed to the octoxy side chain. It can also be observed that there are signals due to the vinyl end groups at $\delta = 5.3$, 5.9, and 6.8. By comparing the integration ratio of these peaks with those of

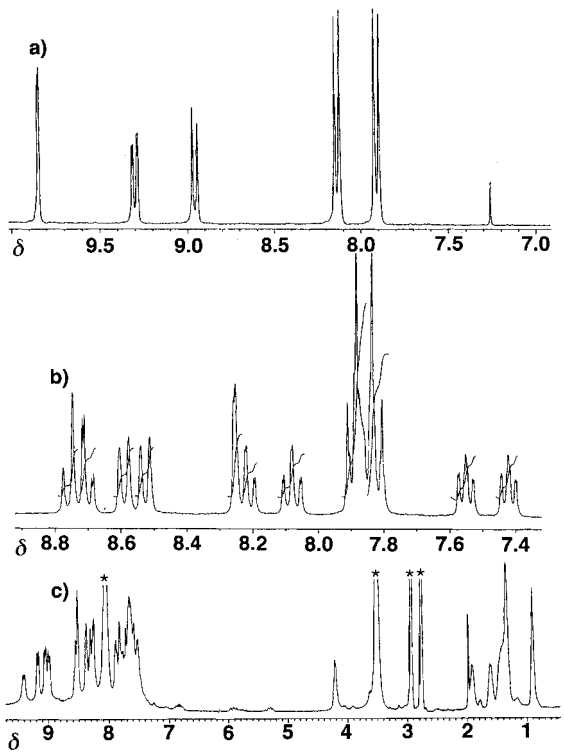

Figure 1. ^{1}H NMR spectra of a) ligand **5** in $CDCl_3$; b) ruthenium complex **7** in CD_3CN; c) polymer **15e** in [D_7]DMF.

Table 1. Synthesis and physical properties of different ruthenium containing polymers with 1,3,4-oxadiazole-substituted bipyridine ligands.

polymer	metal complex monomer	x	y	yield [%][a]	T_d [°C][b]	η_{inh} [dL g^{-1}][c]	μ_h [10^{-4} cm^{2}V^{-1}s^{-1}][d]	μ_e [10^{-4} cm^{2}V^{-1}s^{-1}][d]
13a	**7**	0.1	0.9	85	434	0.61	0.47	0.50
13b	**7**	0.25	0.75	97	416	0.46	0.55	0.57
13c	**7**	0.35	0.65	84	412	0.52	1.8	3.1
13d	**7**	0.5	0.5	83	402	0.32	1.5	3.6
13e	**7**	0.65	0.35	77	401	0.64	4.9	7.9
13f	**7**	1	0	79	424	0.71	5.1	8.3
14a	**8**	0.25	0.75	86	399	0.53	0.21	0.33
14b	**8**	0.5	0.5	74	394	0.31	0.45	1.5
14c	**8**	1	0	76	387	0.30	0.64	3.2

[a] Yield after purification by washing with methanol for 2 days. [b] Onset temperature of decomposition determined by TGA under a nitrogen atmosphere. [c] Inherent viscosity measured in solution in NMP at 30 °C with concentration $c = 0.25$ g dL^{-1}. [d] Charge-carrier mobility measured at an electric field strength of $E = 40$ kV cm^{-1}.

Table 2. Synthesis and physical properties of different ruthenium or rhenium containing polymers based on 1,10-phenanthroline ligands.

polymer	metal complex monomer	x	y	yield [%][a]	T_d [°C][b]	η_{inh} [dL g^{-1}][c]	μ_h [10^{-4} cm^{2}V^{-1}s^{-1}][d]	μ_e (10^{-4} cm^{2}V^{-1}s^{-1}][d]
15a	**10**	0.1	0.9	85	392	0.46	0.8	2.1
15b	**10**	0.2	0.8	87	383	0.44	1.3	2.8
15c	**10**	0.3	0.7	80	372	0.41	1.3	3.0
15d	**10**	0.4	0.6	76	371	0.33	1.5	3.3
15e	**10**	0.5	0.5	75	383	0.40	1.8	3.8
15f	**10**	0.6	0.4	70	382	0.34	2.4	4.6
15g	**10**	1	0	72	392	0.32	3.1	6.5
16a	**11**	0.1	0.9	86	408	0.38	0.4	1.2
16b	**11**	0.2	0.8	83	403	0.36	1.0	1.9
16c	**11**	0.3	0.7	88	410	0.32	1.1	2.4
16d	**11**	0.5	0.5	87	415	0.40	1.4	2.7
16e	**11**	0.7	0.3	78	407	0.32	2.1	4.0

[a] Yield after purification by washing with methanol for 2 days. [b] Onset temperature of decomposition determined by TGA under a nitrogen atmosphere. [c] Inherent viscosities for polymers **15a–g** were measured in solution in NMP at 30 °C with concentration $c = 0.25$ g dL^{-1}. For polymers **16a–e**, they were measured in solution in 1,1,2,2-tetrachloroethane. [d] Charge-carrier mobility measured at an electric field strength of $E = 40$ kV cm^{-1}.

© WILEY-VCH Verlag GmbH, D-69451 Weinheim, 2001
0947-6539/01/0720-4360 $ 17.50+.50/0 *Chem. Eur. J.* **2001**, *7*, No. 20

the methylene units of the alkyl pendant chain, the number average degree of polymerization was estimated to be approximately ten, which corresponds to the number average molecular weight of approximately 12000. The metal content in the polymers was estimated by NMR spectra by comparing the ratio of the protons on the bipyridine units with those of the methylene units. The monomer fed ratio also agrees well with the metal content of the resulting polymers. In the FTIR spectra, all polymers exhibit a characteristic pyridine C=N stretching band at 1600 cm^{-1}. For polymers **13**–**14** (Scheme 3), the C=N and C–O stretching bands for the oxadiazole ring appear at 1576 and 1080 cm^{-1}, respectively. Another absorption band at 831 cm^{-1} is ascribed to the typical C–H out-of-plane bending of the 1,4-disubstituted phenylene units. After the incorporation of the ruthenium complex, a very strong band is found at 841 cm^{-1} corresponding to the P–F stretching of the counter anion. In polymers **16a**–**e**, three strong absorption bands are found at 2015, 1935, and 1892 cm^{-1} corresponding to the CO stretching of the rhenium carbonyl with a *fac* configuration. This is strong evidence for the presence of rhenium complexes on the polymer main chain. These polymers exhibit modest thermal stabilities, and their inherent viscosities are in the range of 0.3–0.7 $dL\,g^{-1}$. It can be seen that the viscosities of polymers **15** and **16** are slightly lower than those of polymers **13** and **14**. This is due to the fact that in monomers **10** and **11**, the bromo groups are quite close to the bulky metal complexes that lower the reactivities of the corresponding monomers. In monomers **7** and **8**, the reaction sites for the palladium coupling reaction are far from the metal center. Nevertheless, optical quality films were obtained by casting or spin coating techniques from polymer solutions.

The electronic absorption spectra of some polymers are shown in Figure 2, Figure 3, and Figure 4. All polymers with the 2,2′-bipyridyl ruthenium moieties show an intense absorption band at 290 nm, which is assigned to the $\pi-\pi^*$ intraligand transition of the bipyridine ligand. The intensity of these peaks increases with increasing metal content in the polymers (Figures 2 and 3). Another strong and broad absorption band is found in the region between 410–450 nm. This is attributed to the $\pi-\pi^*$ electronic transition of the conjugated polymer main chain. In general, it was observed that the absorption maxima of these bands shifted to shorter wavelengths when the metal content was increased. This is because the bulky metal complexes on the main chain inhibit an efficient overlapping of the π-orbitals and thus

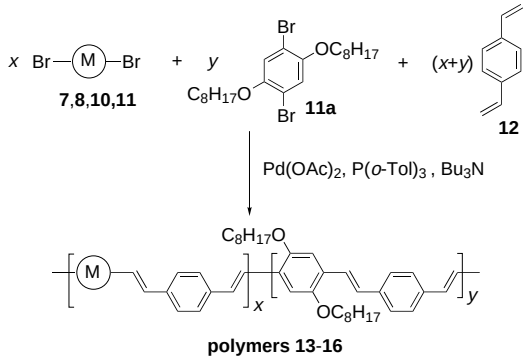

polymers 13-16

Scheme 3. Synthesis of polymers by palladium catalyzed olefinic coupling reactions.

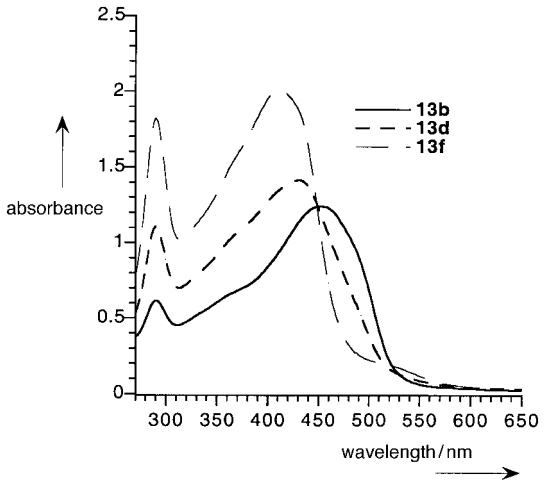

Figure 2. UV/Vis absorption spectra of polymers **13b**,**d**,**f** in solution in DMF.

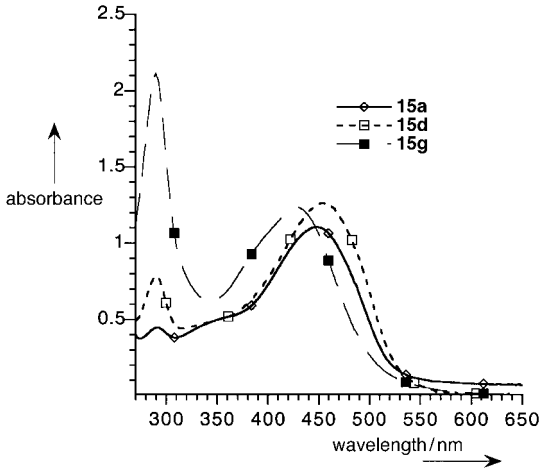

Figure 3. UV/Vis absorption spectra of polymers **15a**,**d**,**g** in solution in DMF.

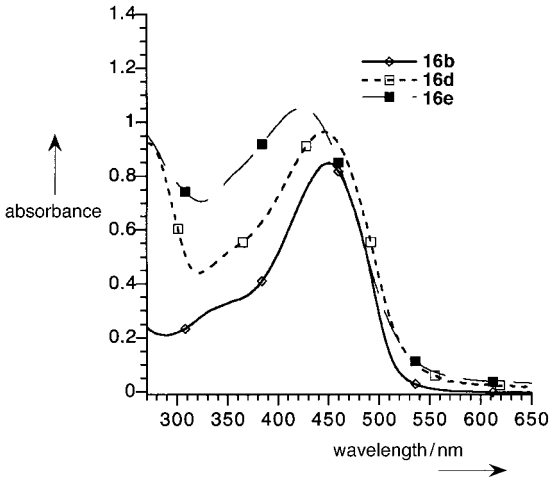

Figure 4. UV/Vis absorption spectra of polymers **16b**,**d**,**e** in solution in 1,1,2,2-tetrachloroethane.

increase the transition energies. In addition, the characteristic d–π* MLCT transitions of the ruthenium or rhenium complexes appear as shoulders at approximately 500 nm. Although the intensity of these MLCT bands increases with increasing amounts of metal complex, it is difficult to correlate their intensities to the metal content in the polymers as a result of the higher absorption coefficient exhibited by the electronic transition of the π-systems.

Electrochemical properties: The electrochemical properties of the polymers were studied by cyclic voltammetry (CV). Figure 5 shows the CV scans of some polymers in different solvent systems; the systems used depend on the polymer

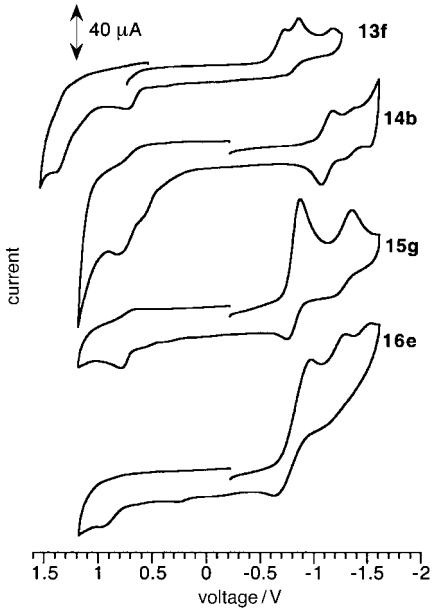

Figure 5. Cyclic voltammograms of polymers **13f**, **14b**, **15g** (in DMF/CH_3CN), and **16e** (in CH_2Cl_2). Tetra-*n*-butylammonium tetrafluoroborate (0.1M) was used as the supporting electrolyte. Glassy carbon was used as the working electrode, and the scan rate was 50 mV s^{-1}.

solubility. As a result of the low solubility of polymers **13**–**15** in acetonitrile, we carried out the CV experiments by adding a few drops of polymer solution in DMF to acetonitrile. However, the scan range was reduced by this method due to the presence of DMF. For polymer **16e**, the CV experiments were carried out in solution in dichloromethane. In the cyclic voltammogram of polymer **13f**, two irreversible reduction processes are observed at −0.8 and −0.95 V in the cathodic scan. These are assigned to the reduction of the polymer main chain, which is considered to involve the addition of electrons to the polymer (n-doping). Such low reduction potential may facilitate the transport of electrons in the polymers. The reduction potentials are significantly lower than those for other unsubstituted bipyridyl ruthenium complexes as a result of the presence of the electron-withdrawing oxadiazole moieties.[18] In the reverse scan, an anodic peak for the undoping process corresponding to the removal of an electron is observed at 0.7 V. In addition, another oxidation process at 1.25 V is assigned to the metal centered $Ru^{III/II}$ couple.

For polymer **14b**, the first reduction process is observed at −0.9 V, which is slightly lower than that in polymer **13f**. This higher reduction potential is attributed to the 4,4′-disubstituted bipyridine main chain with less extended conjugation. Other peaks observed in the cathodic scan originate from the successive reduction of the ligands. In the reverse scan, a similar anodic process is observed at approximately 0.8 V. The phenanthroline based polymers **15g** and **16e** show similar reduction processes in the cathodic scan, and their reduction peaks are widely separated.

Charge-transport properties: Our previous work showed that as a result of the presence of an electron-deficient polymer main chain and other bipyridyl ligands, the electron-carrier mobility of the polymers can be enhanced as they act as extra charge carriers in the charge-transport process.[12] We investigated the role of the metal complexes in charge-transport processes by measuring their charge-carrier mobilities from conventional time-of-flight experiments. The photocurrent pulse shows a featureless decay, which is characteristic for dispersive charge transport with non-Gaussian carrier distribution. Drift mobility was calculated according to Equation (1).

$$\mu = L/t_T E \quad (1)$$

In the equation, L is the film thickness, E is the applied field strength, and t_T is the transit time for charge transport. The electron- and hole-carrier mobilities of the polymers were determined to be of the order of 10^{-4} to 10^{-5} cm^2 V^{-1} s^{-1} (Tables 1 and 2). In general, the charge-carrier mobilities increase with the metal complex content in the polymers. These values are significantly higher than those of the phenyl-substituted or unsubstituted PPVs[19] and polycarbonate doped with oxadiazole derivatives.[20] The enhancement in electron-drift mobilities is possibly due to the presence of oxadiazole moieties in the backbone, as most PPVs are p-type polymers. The carrier mobilities were found to be temperature dependent, and this indicates a thermally activated charge-transport process. From the plot of temperature-dependent charge mobility (Figure 6), the activation energies

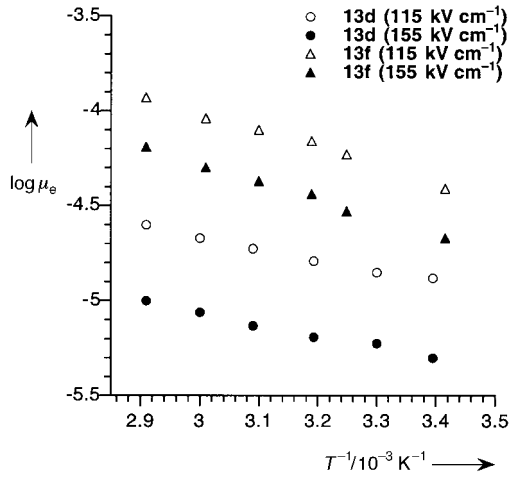

Figure 6. Plot of electron-carrier mobility for polymers **13d**,**f** as a function of temperature under different externally applied electric fields.

© WILEY-VCH Verlag GmbH, D-69451 Weinheim, 2001
0947-6539/01/0720-4362 $ 17.50+.50/0 *Chem. Eur. J.* **2001**, *7*, No. 20

of charge transport were calculated to be approximately 0.1–0.2 eV. Figure 7 shows the plot of electron- and hole-carrier mobilities of some polymers as a function of electric field strength. The graph shows a negative slope, which is

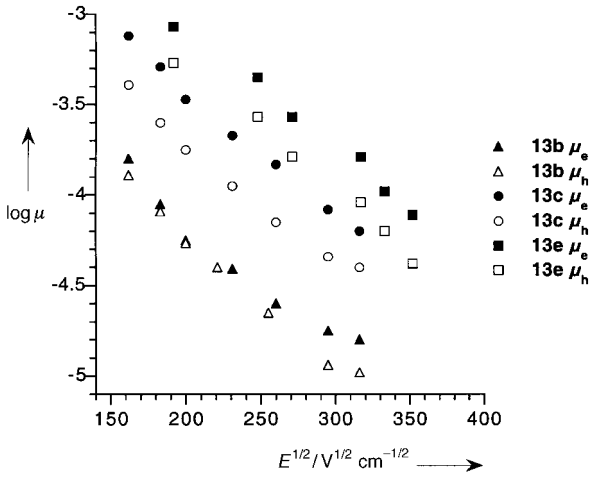

Figure 7. Plot of hole- and electron-carrier mobilities for polymers **13b**,**c**,**e** as a function of externally applied electric field at 298 K.

rationalized as the presence of off-diagonal disorder due to the distribution of distances between molecules in an amorphous polymer system. The charge may hop against the field direction in order to open a faster route for charge transport. As the applied field is increased, "backward jumps" and these "indirect routes" will be inhibited. This process is only favorable under a low-field condition. As the electric field is further increased, this effect will reach a maximum, and the carrier mobilities are dependent on the distortion of the density of hopping states by the applied field. A turning point may be observed in the log μ versus $E^{1/2}$ plot. However, when we increased the electric field further, the polymer films were subjected to dielectric breakdown due to the ionic species in the polymer main chain. From these studies, we suggest that the charge transport could involve inter- or intramolecular hopping processes between the charge carrying species (i.e. metal complexes). Because of the relatively high charge-carrier mobilities, polymers with 5,5′-oxadiazole-substituted bipyridine were selected for detail studies on opto-electronic properties.

Photosensitizing properties: There have been several reports on the use of molecular ruthenium complexes as photosensitizing agents in solar cells or photorefractive materials.[21] The photosensitivity of the polymers should be enhanced by the metal complexes beyond 500 nm, at which the conjugated systems do not absorb. A typical photosensitization process consists of photoexcitation and charge separation. The oxadiazole moieties may facilitate the initial hole–electron separation because of their affinity for electrons. In order to study the photosensitivity of the polymer, a simple two-layered photovoltaic cell with the structure ITO/polymer/C_{60}/Al was constructed. Polymer **13f** was chosen for studies because of its high metal content and charge-carrier mobilities. We were not able to prepare a single-layered photovoltaic cell consisting of a blend of ruthenium containing polymer and C_{60} because the latter is incompatible with the polymer matrix and is also insoluble in the polar solvent medium (DMF) used for spin coating. When excited by light, the charges generated by photoexcitation were separated at the polymer/C_{60} interface. Due to the high electron affinity of C_{60}, the electrons were collected at this layer, and photocurrent was generated as a result. Figure 8a shows the current–voltage characteristics of the photodiode in the dark and under illumination by a xenon arc lamp that simulates solar radiation with an intensity of 100 mW cm^{-2}. Under illumination, the short circuit current and the open circuit voltage are approximately 0.05 mA cm^{-2} and 0.35 V, respectively. The conversion efficiency was estimated to be 0.5%. Figure 8b shows the photocurrent density of the device under different light intensity.

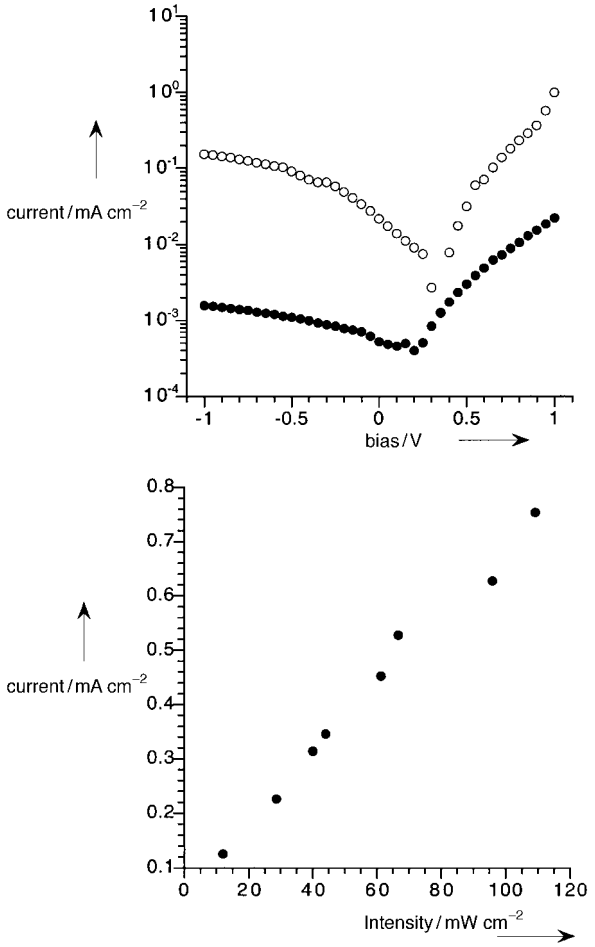

Figure 8. a) Current–voltage characteristics of the ITO/polymer **13f**/C_{60}/Al device in the dark (solid circles) and under 100 mW cm^{-2} illumination (open circles); b) A plot of photocurrent response of the device as a function of irradiated light intensity under a forward bias of 1 V.

Light-emitting properties: Single-layer light-emitting devices ITO/polymer/Al were constructed and they were subjected to a dc voltage under a forward bias condition. The origin of light emission is attributed to the radiative recombination of exciton states, which are formed by the recombination of oppositely charged polarons generated by the injection of

electrons and holes. Table 3 summarizes the light-emitting properties of some polymers. The PL and EL spectra of some polymers are shown in Figure 9. It should be noted that the

Table 3. Performance of some light-emitting devices.

polymer	turn-on voltage [V]	maximum luminance [cd m^{-2}]	external quantum efficiency [%]	$\lambda_{max,em}$ [nm]
13d	8	180	0.08	590, 690[a]
13e	6	220	0.10	710
13f	6	300	0.10	710
14a	6	100	0.05	600, 700[a]
14b	6	150	0.07	690
15b	6.5	90	0.15	570, 710[a]
15e	7	110	0.17	710
16b	7.5	100	0.20	570, 695[a]
16e	7	130	0.21	700

[a] The emission band appears as a shoulder.

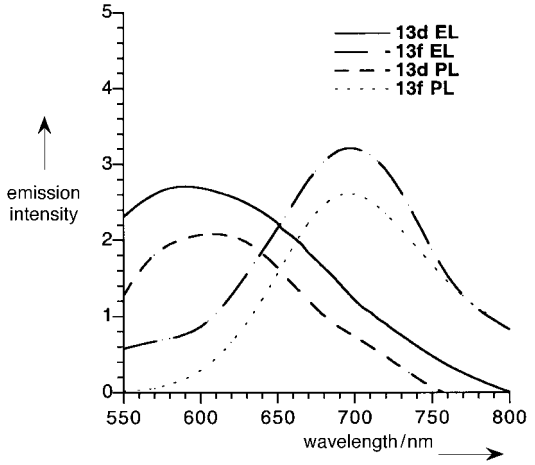

Figure 9. Photoluminescence and electroluminescence spectra of polymers **13d**,**f**.

polymers consist of two light-emitting groups: the π-conjugated system and the metal complex. As a result, they show very broad emission bands in the yellow-red region that extend to very long wavelengths (>750 nm). For polymer **13d**, both PL and EL spectra show major emission bands centered at approximately 590 nm, which originates from the π*–π emission of the conjugated main chain. A small shoulder due to the emission from the MLCT states of the ruthenium complex (π*-d) was also found at approximately 650 nm. On the other hand, polymer **13f** has a higher metal complex content, and its PL and EL spectra were dominated by a relatively narrow emission band centered at 690 nm. No emission from the polymer main chain was observed. This is explained by an energy-transfer process between the conjugated system and the metal complex. After the conjugated main chain has been excited, energy is transferred to the adjacent low-lying MLCT states of the metal complexes. When the metal complex content increases, this "quenching" process is more efficient, and the luminescence spectra are dominated by the MLCT emission. A similar energy-transfer process was also observed in our previously reported conjugated polymers based on ruthenium dipyridophenazine complexes and other systems.[22] The turn-on voltages for the devices were 6 to 8 V. For the polymer with the highest ruthenium content (polymer **13f**), the maximum luminance was determined to be 300 cd m^{-2} at the driving voltage of 28 V. The external quantum efficiency of the devices was in the range between 0.05 and 0.2 %. A typical current–voltage and luminance–voltage plot for polymer **13e** is shown in Figure 10. Despite the relatively short lifetime for these devices (10–20 min under ambient conditions), the design approach of these polymers allows us to fine-tune the electronic and emission properties of the polymers by simply adjusting the amount of metal complex in the polymer.

Conclusion

Two series of conjugated polymers that were functionalized with ruthenium or rhenium diimine complexes have been synthesized. The first series of polymers contains the ruthenium complexes of oxadiazole-substituted 2,2′-bipyridine. The second type of polymers was derived from the ruthenium or rhenium complexes of 1,10-phenanthroline. The use of olefinic coupling reactions allowed the preparation of these polymers directly from their corresponding monomer metal complexes. The uniqueness of the electrochemical and excited-state properties of the complexes was important for the different opto-electronic processes. From the experimental studies, it was shown that these complexes were able to act as photosensitizers, charge-transport species, as well as light emitters. Their physical properties were dependent on the

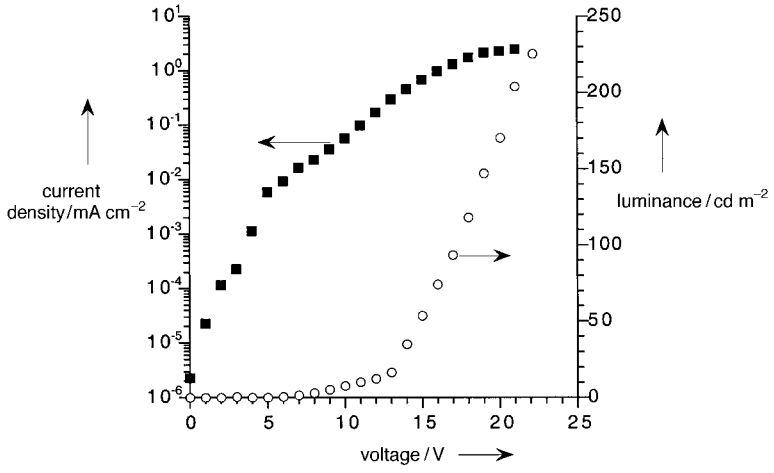

Figure 10. Current–voltage and luminance–voltage characteristics of the light-emitting device ITO/polymer **13e**/Al.

© WILEY-VCH Verlag GmbH, D-69451 Weinheim, 2001
0947-6539/01/0720-4364 $ 17.50+.50/0 *Chem. Eur. J.* **2001**, *7*, No. 20

metal complex content in the polymers. An energy-transfer process between the conjugated main chain and the metal complex moieties was proposed. The investigation of the excited-state nature of the polymer metal complexes and energy-transfer processes constitutes another very intriguing project.

Experimental Section

Materials: All polymerizations were carried out under a nitrogen atmosphere. *N*,*N*-dimethylformamide (DMF) was distilled over CaH_2 under reduced pressure. Pyridine was distilled over CaH_2. Other common organic solvents were analytical grade and used as received unless otherwise stated. Silver trifluoromethanesulfonate, *cis*-dichlorobis(2,2′-bipyridine) ruthenium dihydrate, and bromine were purchased from Aldrich Chemical Co. and used as received. Sodium azide, 4-cyanobromobenzene, ammonium chloride, palladium(II) acetate, tri-*o*-tolylphosphane, tri-*n*-butylamine, and 1,10-phenanthroline monohydrochloride monohydrate were purchased from Lancaster Synthesis Ltd. and used as received. Potassium hexafluorophosphate and rhenium(I) pentacarbonyl chloride were purchased from Strem Chemical Co. The compounds 2,2′-bipyridine-5,5-dicarboxylic acid, 2,2′-bipyridine-4,4′-dicarboxylic acid,[23] 3,8-dibromo-1,10-phenanthroline **9**,[24] 1,4-dibromo-2,5-dioctoxybenzene,[25] and 1,4-divinylbenzene[26] were synthesized according to the literature procedures.

Instruments: ^{1}H and ^{13}C NMR spectra (^{1}H NMR 298 K, ^{13}C NMR 298 K) were collected on a Bruker 300 DPX NMP spectrometer. FTIR spectra (KBr pellet) were collected on a Bio-Rad FTS-7 FTIR spectrometer. UV/Vis absorption spectra were collected on a HP 8453 diode array spectrophotometer. Mass spectrometry was performed on a high-resolution Finnigan MAT-95 mass spectrometer. Thermal analyses were performed on Perkin Elmer DSC7 and TGA7 thermal analyzers. The photoluminescence (PL) and electroluminescence (EL) spectra were collected on an ORIEL MS-257 monochromator equipped with an ANDOR DV420-BV charge-coupled device (CCD) detector. Electrochemical experiments were performed by using a Princeton Applied Research 270 potentiostat with a glassy carbon working electrode and silver/silver chloride reference electrode. Distilled acetonitrile or dichloromethane were used as solvents, and tetrabutylammonium tetrafluoroborate (0.1 M) was used as the supporting electrolyte. A small amount of ferrocene was added as an internal standard.

Synthesis. 1-bromo-4-tetrazoylbenzene 2: A mixture of 4-cyanobromobenzene (1 g, 5.5 mmol), sodium azide (5.7 g, 0.088 mol), ammonium chloride (4.7 g, 0.088 mol), and dry DMF (40 mL) was stirred and heated under reflux for 75 h. The cooled solution was added to dilute hydrochloric acid (150 mL). The precipitate was collected and washed with water and it was recrystallized with methanol. Yield 1.0 g (81 %).

^{1}H NMR (300 MHz, [D$_6$]DMSO): $\delta = 7.99$ (d, $J = 8.5$ Hz, 2H), 7.84 (d, $J = 8.3$ Hz, 2H); ^{13}C NMR (75 MHz, [D$_6$]DMSO): $\delta = 132.4$, 128.8, 128.6, 124.6, 123.6; MS (70 eV, EI): m/z (%): 226 $[M]^+$.

5,5′-Bis[2-(4-bromophenyl)-1,3,4-oxadiazoyl]-2,2′-bipyridine 5: Under a nitrogen atmosphere, a mixture of 2,2′-bipyridine-5,5′-dicarboxylic acid (1.14 g, 4.7 mmol) and thionyl chloride (20 mL) was heated under reflux for 24 h. The excess thionyl chloride was removed by distillation. Compound 1-bromo-4-tetrazoylbenzene (2.3 g, 10 mmol) and dry pyridine (90 mL) were added to the acid chloride formed. The mixture was heated under reflux for another 50 h. After cooling, the mixture was poured into water, and the crude product was washed in hot methanol and then dried under vacuum (2.45 g, 91 % yield).

^{1}H NMR (300 MHz, CF_3COOD-$CDCl_3$): $\delta = 9.85$ (d, $J = 1.6$ Hz, 2H), 9.31 (d, $J = 8.5$ Hz, 2H), 8.97 (d, $J = 8.5$ Hz, 2H), 8.14 (d, $J = 8.6$ Hz, 4H), 7.91 (d, $J = 8.6$ Hz, 4H); ^{13}C NMR (75 MHz, CF_3COOD-$CDCl_3$): $\delta = 169.1$, 149.8, 147.0, 143.6, 135.3, 132.4, 130.8, 126.4, 125.3, 122.5, 120.7, 110.0; FTIR (KBr pellet): $\tilde{\nu} = 1600$, 1576 (C=N), 833 cm^{-1} (1,4-disubstituted phenylene); MS (FAB): m/z (%): 602 $[M]^+$; elemental analysis calcd (%) for $C_{26}H_{14}N_6O_2Br_2$ (602.2): C 51.85, H 2.34, N 13.95; found: C 51.90, H 2.42, N 13.95.

4,4′-Bis[2-(4-bromophenyl)-1,3,4-oxadiazoyl]-2,2′-bipyridine 6: This compound was synthesized according to a similar procedure as for compound **5** except that 2,2′-bipyridine-4,4′-dicarboxylic acid was used instead. Yield 2.5 g (93 %).

^{1}H NMR (300 MHz, CF_3COOD-$CDCl_3$): $\delta = 9.66$ (d, $J = 1.0$ Hz, 2H), 9.29 (d, $J = 5.6$ Hz, 2H), 8.72 (d, $J = 5.6$ Hz, 2H), 8.15 (d, $J = 8.6$ Hz, 4H), 7.89 (d, $J = 8.6$ Hz, 4H); ^{13}C NMR (75 MHz, CF_3COOD-$CDCl_3$): $\delta = 170.1$, 150.1, 149.4, 139.1, 135.6, 132.7, 131.1, 127.0, 123.1, 121.2; FTIR (KBr pellet): $\tilde{\nu} = 1602$, 1574 (C=N), 1075 (C–O stretching), 835 cm^{-1} (1,4-disubstituted phenylene); MS (70 eV, EI): m/z (%): 602 $[M]^+$; elemental analysis calcd (%) for $C_{26}H_{14}N_6O_2Br_2$ (602.2): C 51.85, H 2.34, N 13.95; found: C 51.91, H 2.48, N 13.55.

5,5′-Bis[2-(4-bromophenyl)-1,3,4-oxadiazoyl]-2,2′-bipyridine ruthenium(II) bis(2,2′-bipyridyl) hexafluorophosphate 7: Under a nitrogen atmosphere, silver trifluoromethanesulfonate (0.99 g, 3.8 mmol) was added to a solution of *cis*-dichlorobis(2,2′-bipyridine)ruthenium dihydrate (1 g, 1.9 mmol) in acetone (200 mL). The solution was stirred at room temperature for 2 h, and the silver chloride formed was filtered with a pad of Celite. The filtrate was evaporated to dryness to give $[Ru(bpy)_2(acetone)_2(SO_3CF_3)_2]$ (1.37 g, 90 % yield). The triflate salt was added to a solution of **5** (2.1 g, 3.4 mmol) in DMF (6 mL), and the solution was heated at 120 °C for 12 h. The solution was filtered, and the filtrate was added to an aqueous solution of KPF_6. The product was recrystallized by using a mixture of acetonitrile/diethyl ether and was collected as a reddish brown solid (1.95 g, 77 % yield).

^{1}H NMR (300 MHz, CD_3CN): $\delta = 8.74$ (d, $J = 8.5$ Hz, 2H), 8.68 (d, $J = 8.5$ Hz, 2H), 8.60 (d, $J = 8.1$ Hz, 2H), 8.53 (d, $J = 8.1$ Hz, 2H), 8.25–8.19 (m, 4H), 8.05 (t, $J = 8.0$ Hz, 2H), 7.90–7.87 (m, 8H), 7.83–7.80 (m, 4H), 7.55 (t, $J = 6.1$ Hz, 2H), 7.42 (t, $J = 6.1$ Hz, 2H); ^{13}C NMR (75 MHz, CD_3CN): $\delta = 165.9$, 161.8, 159.3, 158.2, 157.9, 153.4, 153.2, 150.4, 139.4, 139.3, 135.7, 133.8, 129.6, 128.8, 128.7, 127.7, 126.7, 125.6, 125.1, 123.4; FTIR (KBr pellet): $\tilde{\nu} = 1602$, 1559 (C=N), 1081 (C–O), 844 cm^{-1} (P–F stretching); UV/Vis (CH_3CN): λ_{max} (ε) = 290 (83 000), 360 (62 000), 440 (12 000), 530 nm (5800 dm^3 mol^{-1} cm^{-1}); MS (FAB): m/z (%): 1161 $[M - PF_6]^+$, 1016 $[M - 2PF_6]^+$; elemental analysis calcd (%) for $C_{46}H_{30}N_{10}O_2Br_2RuP_2F_{12}$ (1304.4): C 42.25, H 2.31, N 10.71; found: C 42.60, H 2.60, N 10.42.

4,4′-Bis[2-(4-bromophenyl)-1,3,4-oxadiazoyl]-2,2′-bipyridine ruthenium(II) bis(2,2′-bipyridyl) hexafluorophosphate 8: The synthetic procedure was similar to that for **7** except that ligand **6** (1.3 g, 4.7 mmol) was used instead. Yield 1.7 g (66 %).

^{1}H NMR (300 MHz, CD_3CN): $\delta = 8.88$ (m, 8H), 8.26 (m, 6H), 8.05 (d, $J = 6.1$ Hz, 2H), 7.97 (m, 6H), 7.89 (d, $J = 5.4$ Hz, 2H), 7.89 (d, $J = 5.4$ Hz, 2H), 7.76 (d, $J = 5.6$ Hz, 2H), 7.59 (t, $J = 3.1$ Hz, 2H), 7.53 (t, $J = 7.0$ Hz, 2H); ^{13}C NMR (75 MHz, CD_3CN): $\delta = 166.9$, 166.5, 163.1, 159.0, 157.9, 157.7, 154.1, 153.0, 152.7, 149.2, 139.4, 133.8, 133.1, 129.9, 128.9, 128.8, 127.8, 125.5, 125.1, 123.6, 122.4; FTIR (KBr pellet): $\tilde{\nu} = 1600$, 1562 (C=N), 1079 (C–O), 841 cm^{-1} (P–F stretching); UV/Vis (CH_3CN): λ_{max} (ε) = 292 (76 000), 360 (14 000), 480 nm (15 000 dm^3 mol^{-1} cm^{-1}); MS (FAB): m/z (%): 1161 $[M - PF_6]^+$, 1016 $[M - 2PF_6]^+$; elemental analysis calcd (%) for $C_{46}H_{30}N_{10}O_2Br_2RuP_2F_{12}$ (1307.6): C 42.25, H 2.31, N 10.71; found: C 42.30, H 2.63, N 10.92.

3,8-Dibromo-1,10-phenanthroline ruthenium(II) bis(2,2′-bipyridyl) hexafluorophosphate 10: Under a nitrogen atmosphere, silver trifluoromethanesulfonate (0.24 g, 0.96 mmol) was added to a solution of *cis*-dichlorobis(2,2′-bipyridine)ruthenium dihydrate (0.25 g, 0.48 mmol) in acetone (50 mL). The solution was stirred at room temperature for 2 h, and the silver chloride formed was filtered with a pad of Celite. After evaporation of the solvent, the triflate salt $[Ru(bpy)_2(acetone)_2(SO_3CF_3)_2]$ was added to a solution of 3,8-dibromo-1,10-phenanthroline **9** (90 mg, 0.28 mmol) in DMF (3 mL), and the solution was heated at 140 °C for 24 h. The filtered solution was added to an aqueous solution of KPF_6. The product was recrystallized by using a mixture of acetone/diethyl ether and was collected as a dark red solid (0.38 g, 75 %).

^{1}H NMR (300 MHz, CD_3CN): $\delta = 8.84$ (d, $J = 1.8$ Hz, 2H), 8.50 (t, $J = 7.5$ Hz, 4H), 8.19 (d, $J = 1.2$ Hz, 2H), 8.16–7.98 (m, 6H), 7.75 (d, $J = 6.1$ Hz, 2H), 7.65 (d, $J = 5.6$ Hz, 2H), 7.42 (t, $J = 6.3$ Hz, 2H), 7.27 (t, $J = 6.6$ Hz, 2H); ^{13}C NMR (75 MHz, CD_3CN): $\delta = 158.3$, 157.9, 154.6, 153.4, 153.1, 147.1, 140.0, 139.2, 139.1, 132.5, 129.5, 128.7, 128.4, 125.4, 124.2, 122.1; FTIR (KBr pellet): 1604 (C=N), 841 cm^{-1} (P–F stretching); UV/Vis (CH_3CN): λ_{max} (ε) = 248 (36 000), 292 (54 000), 448 nm (11 000 dm^3 mol^{-1} cm^{-1}); MS (FAB): m/z (%): 897 $[M - PF_6]^+$, 752 $[M - 2PF_6]^+$; elemental analysis calcd

(%) for $C_{32}H_{22}N_6Br_2RuP_2F_{12}$ (1041.4): C 36.91, H 2.13, N 8.07; found: C 37.08, H 2.46, N 8.27.

3,8-Dibromo-1,10-phenanthroline rhenium(I) tricarbonyl chloride 11: Compound 3,8-dibromo-1,10-phenanthroline **9** (40 mg, 0.12 mmol) and rhenium(I) pentacarbonyl chloride (40 mg, 0.12 mmol) were added to toluene (20 mL) under a nitrogen atmosphere. The solution was heated under reflux for 2 h. After cooling, the orange-yellow solid was filtered, washed with toluene and diethyl ether, and dried in vacuum (60 mg, 78% yield). ^{1}H NMR (300 MHz, $CDCl_3$): $\delta = 9.42$ (d, $J = 1.8$ Hz, 2H), 8.71 (d, $J = 1.9$ Hz, 2H), 7.98 (s, 2H); ^{13}C NMR (75 MHz, $CDCl_3$): $\delta = 157.6$, 154.4, 149.3, 146.7, 144.5, 139.9, 132.2, 127.8, 122.1; FTIR (KBr pellet): $\tilde{\nu} = 2015$, 1935, 1892 (metal carbonyl CO stretching), 1591 cm^{-1} (C=N); UV/Vis ($CHCl_3$): λ_{max} (ε) = 248 (33000), 292 (30000), 335 (17000), 400 nm (4,300 dm^{3}mol^{-1}cm^{-1}); MS (FAB): m/z (%): 644 $[M]^+$, 613 $[M-Cl]^+$; elemental analysis calcd (%) for $C_{15}H_6N_2O_3ClBr_2Re$ (643.7): C 27.99, H 0.94, N 4.35; found: C 28.18, H 1.02, N 4.28.

Palladium catalyzed polymerization: The synthesis of polymer **13d** was performed as in the general procedure. Divinylbenzene **12** (41 mg, 0.315 mmol), ruthenium complex **7** (0.206 g, 0.158 mmol), 1,4-dibromo-2,5-dioctoxybenzene **11** (78 mg, 0.158 mmol), palladium(II) acetate (2.8 mg, 4 mol%), and tri-*o*-tolylphosphane (38 mg, 0.4 equiv) were added to a 25 mL round-bottomed flask under a nitrogen atmosphere. DMF (5 mL) was added by means of a syringe, and the solution was stirred until all the solid had dissolved. Tri-*n*-butylamine (0.22 mL) was added, and the solution was stirred at 100 °C for 24 h. The solution was poured into methanol, and the polymer was washed with methanol in a Soxhlet extractor for 2 days. The polymer was collected as a dark-brown solid. (0.27 g, 83% yield).

Physical characterization: The polymer films for charge-carrier mobility measurements were prepared by casting a polymer solution on an indium-tin-oxide coated glass slide, and the solvent was evaporated slowly. The typical thickness of the polymer film was approximately 0.5 – 1.0 μm. A thin layer of gold electrode (100 – 120 Å) was coated on the polymer film surface by thermal evaporation under high vacuum (10^{-6} mbar). The charge-carrier mobility was determined by the time-of-flight method.[27] A Laser Science VSL-337 nitrogen laser was used to generate a pulsed laser source [wavelength = 337.1 nm, pulse energy = 120 μJ, and pulse width full width at half-maximum (fwhm) = 3 ns]. The transient photocurrent was monitored by an oscilloscope. The heterojunction photodiode was constructed by subliming a layer of C_{60} (50 nm) onto a polymer film (70 nm) coated on an ITO glass slide. A layer of aluminum electrode (120 nm) was coated on the surface by vacuum evaporation. The photocurrent was measured with a Keithley 238 sourcemeter. An ORIEL xenon arc lamp (150 W) that simulated solar radiation was used as the light source. The irradiation light intensity was 100 mW cm^{-2}.

Acknowledgements

This project was substantially supported by The Research Grants Council of The Hong Kong Special Administrative Region, China (Project Nos. HKU 7093/97P, HKU 7090/98P, and 7096/00P). Partial financial support from The Committee on Research and Conference Grants (University of Hong Kong) is also acknowledged. P.K.N, S.H.C, and L.S.M.L. would like to thank The Graduate School, University of Hong Kong for the award of their studentships. We also thank Prof. Wing Tak Wong for his assistance in the CV experiments.

[1] *Macromolecule-Metal Complexes* (Eds.: F. Ciardelli, E. Tsuchida, D. Wöhrle), Springer, Berlin, **1996**.

[2] J. H. Burroughes, D. D. C. Bradley, A. R. Brown, R. N. Marks, K. Mackay, R. H. Friend, P. L. Burns, A. B. Holmes, *Nature* **1990**, *347*, 539.

[3] *Handbook of Conducting Polymers*, 2nd ed. (Eds.: T. A. Skotheim, R. L. Elsenbaumer, J. R. Reynolds), Marcel Dekker, New York, **1998**.

[4] a) N. Tessler, G. J. Denton, R. H. Friend, *Nature* **1996**, *382*, 695; b) F. Hide, M. A. Diaz-Garcia, B. J. Schwartz, M. R. Andersson, Q. Pei, A. J. Heeger, *Science* **1996**, *273*, 1833.

[5] a) G. Yu, C. Zhang, A. J. Heeger, *Appl. Phys. Lett.* **1994**, *64*, 1540; b) J. J. M. Halls, C. A. Walsh, N. C. Greenham, E. A. Marseglia, R. H. Friend, S. C. Moratti, A. B. Holmes, *Nature* **1995**, *376*, 498; c) G. Yu, A. J. Heeger, *J. Appl. Phys.* **1995**, *78*, 4510; d) J. J. M. Halls, K. Pichler, R. H. Friend, S. C. Moratti, A. B. Holmes, *Appl. Phys. Lett.* **1996**, *68*, 3120.

[6] a) Y. Yang, A. J. Heeger, *Nature* **1994**, *372*, 344; b) Z. Bao, A. Dodabalapur, A. J. Lovinger, *Appl. Phys. Lett.* **1996**, *69*, 4108; c) H. Sirringhaus, N. Tessler, R. H. Friend, *Science* **1998**, *280*, 1741.

[7] *Semiconducting Polymers-Chemistry, Physics and Engineering* (Eds.: G. Hadziioannou, P. F. van Hutten), WILEY-VCH, Weinheim, **2000**.

[8] a) S. C. Yu, X. Gong, W. K. Chan, *Macromolecules* **1998**, *31*, 5639; b) S. C. Yu, S. Hou, W. K. Chan, *Macromolecules* **1999**, *32*, 5251; c) W. K. Chan, P. K. Ng, X. Gong, S. Hou, *J. Mater. Chem.* **1999**, *9*, 2103; d) S. C. Yu, S. Hou, W. K. Chan, *Macromolecules* **2000**, *33*, 3529; e) L. S. M. Lam, S. H. Chan, W. K. Chan, *Macromol. Rapid Commun.* **2000**, *21*, 1081.

[9] W. E. Jones, Jr., L. Hermans, B. Jiang in *Multimetallic and Macromolecular Inorganic Photochemistry* (Eds.: V. Ramamurthy, K. S. Schanze), Marcel Dekker, New York, **1999**, p. 1.

[10] a) K. Kalyanasundaram, *Coord. Chem. Rev.* **1982**, *46*, 159; b) A. Juris, V. Balzani, F. Barigelletti, S. Campagna, P. Belser, A. Von Zelewsky, *Coord. Chem. Rev.* **1988**, *84*, 85.

[11] For example: a) L. Trouillet, A. De Nicola, S. Guillerez, *Chem. Mater.* **2000**, *12*, 1611; b) K. D. Ley, C. E. Whittle, M. D. Bartkerger, K. S. Schanze, *J. Am. Chem. Soc.* **1997**, *119*, 3423; c) K. D. Ley, K. S. Schanze, *Coord. Chem. Rev.* **1998**, *171*, 287; d) Q. Wang, L. M. Wang, L. Yu, *J. Am. Chem. Soc.* **1998**, *120*, 12860; e) B. Wang, M. R. Wasielewski, *J. Am. Chem. Soc.* **1997**, *119*, 12; f) C. G. Cameron, P. G. Pickup, *Chem. Commun.* **1997**, 303; g) S. C. Rasmussen, D. W. Thompson, V. Singh, J. D. Petersen, *Inorg. Chem.* **1996**, *35*, 3449.

[12] a) W. K. Chan, X. Gong, W. Y. Ng, *Appl. Phys. Lett.* **1997**, *71*, 2919; b) W. K. Chan, P. K. Ng, X. Gong, S. Hou, *Appl. Phys. Lett.* **1999**, *75*, 3920.

[13] a) V. W. W. Yam, C. L. Chan, S. W. K. Choi, K. M. C. Wong, E. C. C. Cheng, S. C. Yu, P. K. Ng, W. K. Chan, K. K. Cheung, *Chem. Commun.* **2000**, 53; b) C. T. Wong, W. K. Chan, *Adv. Mater.* **1999**, *11*, 455; c) W. Y. Ng, X. Gong, W. K. Chan, *Chem. Mater.* **1999**, *11*, 1165; d) M. A. Baldo, S. Lamansky, P. E. Burrows, M. E. Thompson, S. R. Forrest, *Appl. Phys. Lett.* **1999**, *75*, 4; e) E. S. Handy, A. J. Pai, M. F. Rubner, *J. Am. Chem. Soc.* **1999**, *121*, 3525; f) X. Gong, P. K. Ng, W. K. Chan, *Adv. Mater.* **1998**, *10*, 1337; g) C. H. Lyons, E. D. Abbas, J.-K. Lee, M. F. Rubner, *J. Am. Chem. Soc.* **1998**, *120*, 12100; h) Y. Ma, H.-Y. Chao, Y. Wu, S. T. Lee, W.-Y. Yu, C.-M. Che, *Chem. Commun.* **1998**, 2491; i) Y. Ma, H. Zhang, J. Shen, C. M. Che, *Synth. Met.* **1998**, *94*, 245; j) J.-K. Lee, D. Yoo, M. F. Rubner, *Chem. Mater.* **1997**, *9*, 1710; k) X. T. Tao, H. Suzuki, T. Watanabe, S. H. Lee, S. Miyata, H. Sasabe, *Appl. Phys. Lett.* **1997**, *70*, 1503.

[14] a) M. A. Baldo, D. F. O'Brien, Y. You, A. Shoustikov, S. Sibley, M. E. Thompson, S. R. Forrest, *Nature* **1998**, *395*, 151; b) D. F. O'Brien, M. A. Baldo, M. E. Thompson, S. R. Forrest, *Appl. Phys. Lett.* **1999**, *74*, 442.

[15] B. Schulz, M. Bruma, L. Brehmer, *Adv. Mater.* **1997**, *9*, 601.

[16] For example: a) Q. Pei, Y. Yang, *Adv. Mater.* **1995**, *7*, 559; b) E. Buchwald, M. Meier, S. Karg, P. Pösch, H.-W. Schmidt, P. Strohriegl, W. Rieß, M. Schwoerer, *Adv. Mater.* **1995**, *7*, 839; c) Z. Peng, Z. Bao, M. E. Galvin, *Adv. Mater.* **1998**, *10*, 680; d) S. Yin, J. Peng, W. Huang, X. Liu, W. Li, B. He, *Synth. Met.* **1998**, *93*, 193.

[17] N. Tamoto, C. Adachi, K. Nagai, *Chem. Mater.* **1997**, *9*, 1077.

[18] C. M. Elliott, E. J. Hershenhart, *J. Am. Chem. Soc.* **1982**, *104*, 7519.

[19] a) P. M. Borsenberger, L. Pautmeier, H. Bässler, *J. Chem. Phys.* **1991**, *94*, 5447; b) A. Y. Kryukov, A. C. Saidov, A. V. Vannikov, *Thin Solid Films* **1992**, *209*, 84.

[20] H. Tokuhisa, M. Era, T. Tsutsui, S. Saito, *Appl. Phys. Lett.* **1995**, *66*, 3433.

[21] a) G. Wolfbauer, A. M. Bond, G. B. Deacon, D. R. MacFarlane, L. Spiccia, *J. Am. Chem. Soc.* **2000**, *122*, 130; b) P. H. Xie, Y. J. Hou, T. X. Wei, B. W. Zhang, Y. Cao, C. H. Huang, *Inorg. Chim. Acta.* **2000**, *308*, 73; c) M. Yanagida, L. P. Singh, K. Sayama, K. Hara, R. Katoh, A. Islam, H. Sugihara, H. Arakawa, M. K. Nazeeruddin, M. Gratzel, *J. Chem. Soc. Dalton Trans.* **2000**, 2817; d) Z. Peng, A. R. Gharavi, L. Yu, *Appl. Phys. Lett.* **1996**, *69*, 4002.

 © WILEY-VCH Verlag GmbH, D-69451 Weinheim, 2001 0947-6539/01/0720-4366 $ 17.50+.50/0

[22] P. K. Ng, X. Gong, W. T. Wong, W. K. Chan, *Macromol. Rapid Commun*. **1997**, *18*, 1009.
[23] A. R. Oki, R. J. Morgan, *Syn. Commun*. **1995**, *25*, 4093.
[24] D. Tzalis, Y. Tor, S. Failla, J. S. Siegel, *Tetrahedron Lett*. **1995**, *36*, 3489.
[25] A. Greiner, H. Martelock, A. Noll, N. Siegfried, W. Heitz, *Polymer* **1991**, *32*, 1857.
[26] B. T. Strey, *J. Polym. Sci. Polym. Lett. Ed*. **1965**, 265.
[27] W. E. Spear, *Proc. Phys. Soc. London Sect. B* **1975**, *70*, 669.

Received: March 16, 2001 [F3135]